

Neuroprotective effect of immunomodulatory peptides in rats with traumatic spinal cord injury

<https://doi.org/10.4103/1673-5374.301485>

Date of submission: May 11, 2020

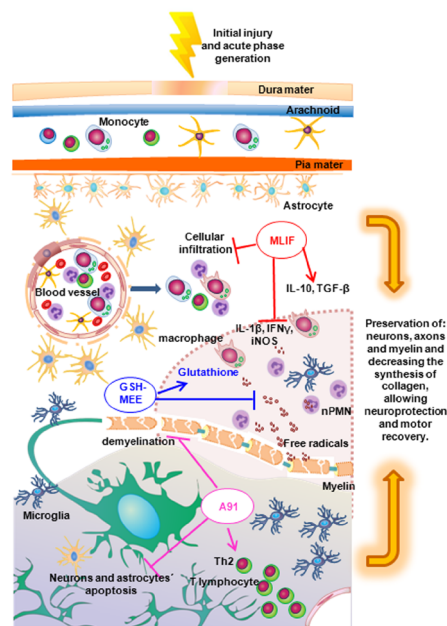
Date of decision: June 21, 2020

Date of acceptance: September 2, 2020

Date of web publication: December 12, 2020

Dulce Parra-Villamar¹, Liliana Blancas-Espinoza¹, Elisa Garcia-Vences^{2,3}, Juan Herrera-García¹, Adrian Flores-Romero^{2,3}, Alberto Toscano-Zapien¹, Jonathan Vilchis Villa¹, Rodríguez Barrera-Roxana^{2,3}, Soria Zavala Karla^{1,2}, Antonio Ibarra^{2,3,*}, Raúl Silva-García^{1,*}

Graphical Abstract The initial lesion causes an exacerbated immune response, which is modulated by peptides at different events, favoring neuroprotection and motor recovery [Decreases (↔), increases (→)].



Abstract

Several therapies have shown obvious effects on structural conservation contributing to motor functional recovery after spinal cord injury (SCI). Nevertheless, neither strategy has achieved a convincing effect. We purposed a combined therapy of immunomodulatory peptides that individually have shown significant effects on motor functional recovery in rats with SCI. The objective of this study was to investigate the effects of the combined therapy of monocyte locomotion inhibitor factor (MLIF), A91 peptide, and glutathione monoethyl ester (GSH-MEE) on chronic-stage spinal cord injury. Female Sprague-Dawley rats underwent a laminectomy of the T9 vertebra and a moderate contusion. Six groups were included: sham, PBS, MLIF + A91, MLIF + GSH-MEE, A91 + GSH-MEE, and MLIF + A91 + GSH-MEE. Two months after injury, motor functional recovery was evaluated using the open field test. Parenchyma and white matter preservation was evaluated using hematoxylin & eosin staining and Luxol Fast Blue staining, respectively. The number of motoneurons in the ventral horn and the number of axonal fibers were determined using hematoxylin & eosin staining and immunohistochemistry, respectively. Collagen deposition was evaluated using Masson's trichrome staining. The combined therapy of MLIF, A91, and GSH-MEE greatly contributed to motor functional recovery and preservation of the medullary parenchyma, white matter, motoneurons, and axonal fibres, and reduced the deposition of collagen in the lesioned area. The combined therapy of MLIF, A91, and GSH-MEE preserved spinal cord tissue integrity and promoted motor functional recovery of rats after SCI. This study was approved by the National Commission for Scientific Research on Bioethics and Biosafety of the Instituto Mexicano del Seguro Social under registration number R-2015-785-116 (approval date November 30, 2015) and R-2017-3603-33 (approval date June 5, 2017).

Key Words: glutathione monoethyl ester; monocyte locomotion inhibitor factor; motor functional recovery; neuroprotection; neurorestoration; peptides; protective autoimmunity; spinal cord injury

Chinese Library Classification No. R453; [364.7]; R741

¹Unidad de Investigación Médica en Inmunología, Hospital de Pediatría, Centro Médico Nacional Siglo XXI; Instituto Mexicano del Seguro Social; Ciudad de México, México; ²Centro de Investigación en Ciencias de la Salud (CICSA), Facultad de Ciencias de la Salud, Universidad Anáhuac México, Campus Norte, Huixquilucan, Edo de México, México; ³Centro de Investigación del Proyecto Camina A.C, Ciudad de México, México

*Correspondence to: Antonio Ibarra, MD, MSc, DSc, jose.ibarra@anahuac.mx; Raúl Silva-García, MSc, DSc, silgarrul@yahoo.com.mx. <https://orcid.org/0000-0003-2489-4689> (Antonio Ibarra); <https://orcid.org/0000-0002-6178-9063> (Raúl Silva-García)

Funding: This study was supported by Fondo de Investigación en Salud of the Instituto Mexicano del Seguro Social (IMSS), under the support No. FIS/IMSS/PROT/G17/1676 and FIS/IMSS/PROT/G18/1825 and the scholarship granted to the students of Master's degree by Consejo Nacional de Ciencia y Tecnología (CONACYT) and IMSS.

How to cite this article: Parra-Villamar D, Blancas-Espinoza L, Garcia-Vences E, Herrera-García J, Flores-Romero A, Toscano-Zapien A, Villa JV, Barrera-Roxana R, Karla SZ, Ibarra A, Silva-García R (2021) Neuroprotective effect of immunomodulatory peptides in rats with traumatic spinal cord injury. *Neural Regen Res* 16(7):1273-1280.

Introduction

Spinal cord injury (SCI) has a global incidence of 250,000 to 500,000 new cases annually and is considered a public health problem due to its economic and social repercussions (Wilson et al., 2020). Ninety percent of SCIs occur due to traumatic causes, and in these cases, the damage to the tissue is induced by the primary event and the secondary events triggered after injury. These mechanisms exert their degenerative effects during different stages of damage (acute, sub-acute, and chronic phases) (Oyinbo, 2011).

The primary damage occurs mechanically due to an impact, laceration, or transection, and it is irreversible, resulting in compression or tearing, limiting blood supply and causing a rupture of the hematoespinal barrier at the site of injury (Dalbayrak et al., 2015). The primary event induces tissue destruction, destabilization of neuronal and endothelial membrane (Profyris et al., 2004), and biochemical and cellular actions that lead to the secondary damage. Simultaneously, resident and peripheral cells are activated and accompanied by ionic deregulation events, loss of homeostasis (Hille and Catterall, 1999; Oyinbo, 2011), excitotoxicity, lipid peroxidation (LP), and synthesis of cytokines and enzymes (Xu et al., 2004; Hall et al., 2016; Vilchis et al., 2019; Bloom et al., 2020). These events, in combination with others, cause diverse morphological alterations, such as cavitation formation, axonal demyelination, glial scar (GS) formation, and collagen IV synthesis which represent the mechanical aspects that restrict axonal regeneration (Liesi and Kaupila, 2002; Fitch and Silver, 2008; Chen and Zhu, 2016).

Secondary events may become chronic producing more neuronal degeneration that further worsens patient's health, thus decreasing the quality of life (Rowland et al., 2008; Moghaddam et al., 2015).

In recent years, neuroprotective therapies (e.g., methylprednisolone, erythropoietin, immunomodulation), have been implemented to reduce destructive events following SCI. Such therapies are aimed at repairing damaged neural tissue or regenerating new neural tissue, neutralizing toxic mediators or increasing tissue resistance to toxicity triggered by SCI, avoiding expansion of the lesion, and promoting motor functional recovery (Faden and Stoica, 2007; Bains and Hall, 2012). Most of the drugs that have been studied as possible neuroprotective agents are only focused on a single type of damage, and these treatments have even been customized according to the specific mechanisms of the primary lesion (Hilton et al., 2017). The multiple drugs that have been suggested as a possible treatment for SCI include immunomodulatory peptides, which in recent decades have been identified as potential agents for treatment of some central nervous system (CNS) pathologies (Guizar-Sahagun et al., 2005; del Rayo-Garrido et al., 2013; Bermeo et al., 2015). Our group used several peptides, including monocyte locomotion inhibitor factor (MLIF), A91 peptide and glutathione monoethyl ester (GSH-MEE), to treat SCI in murine models. MLIF is a pentapeptide (Met-Gln-Cys-Asn-Ser) produced by *Entamoeba histolytica*. A91 peptide corresponds to the immunodominant epitope of sequence 87–99 of the myelin basic protein with a lysine substituted by an alanine at position 91 (–Val-His-Phe-Phe-Ala-Asn-Ile-Val-Thr-Pro-Arg-Thr-Pro–). Glutathione monoethyl ester is a membrane permeable compound [γ -Glu-Cys-Gly-OEt (GSH-MEE)] that increases the intracellular concentrations of glutathione (GSH) (Martíñon et al., 2007; del Rayo-Garrido et al., 2013). Each of these peptides, when individually administered, has been shown to exhibit the ability to modulate some of the secondary events triggered by SCI, favoring motor function recovery (Guizar-Sahagun et al., 2005; del Rayo-Garrido et al., 2013; Bermeo et al., 2015).

MLIF diminishes the migration of inflammatory cells and their ability to produce free radicals. Additionally, this peptide enhances the Th2 response and upregulates interleukin-10 (IL-10) and transforming growth factor-beta (TGFB) expression (Bermeo et al., 2013). On the other hand, GSH-MEE is an excellent antioxidant that neutralizes free radicals (FR) diminishing LP. Likewise, GSH-MEE increases the activation, proliferation, and cellular differentiation of immune cells (especially T-lymphocytes) and promotes the upregulation of IL-2 and TGFB (Martíñon et al., 2007). After 3–5 days of immunization, A91 peptide induces a Th2 response that modulates inflammatory response, diminishing LP and apoptosis. Aside from this, the induced Th2 response is capable of producing neurotrophic factors and promoting neurogenesis and axonal regeneration (Martíñon et al., 2007; Rodríguez-Barrera et al., 2020). The beneficial effects of A91 peptide immunization are expected to initiate their action until the subacute phase of injury. The neural tissue is unprotected during the acute stage. The addition of MLIF and GSH-EE can protect the tissue from the beginning of injury by reducing inflammation, LP, and apoptosis, thereby enabling an earlier and better motor function recovery (Rodríguez-Barrera et al., 2013). Furthermore, during the acute phase, MLIF and GSH-MEE support and enhance the anti-A91 response. We anticipated that the separate actions of MLIF and GSH-MEE, from the beginning, will potentiate their effect on inflammation, FR production, and anti-A91 stimulation. In a continuum effect, A91-induced response will provide protective effects during the subacute stage, contributing to restoration of injured neural tissue.

Therefore, the general objective of this work was to evaluate the neuroprotection induced by the combination of these immunomodulatory peptides in animal models of moderate SCI in terms of motor function recovery, the preservation of medullary parenchyma, ventral horn neurons and myelin, and the presence of collagen and axonal fibres at the site of injury.

Materials and Methods

Ethical considerations

Rats were handled according to the National Institutes of Health (NIH) guidelines for handling laboratory animals, the Norma Oficial Mexicana NOM-062-ZOO-1999 technical specifications for the production, care, and use of laboratory animals, the Official Mexican Standard NOM-033-ZOO-1995 on the humane slaughter of domestic and wild animals, and the Procedure Manual and Recommendations for Laboratory Animal Research from Instituto Mexicano del Seguro Social. In addition, the National Commission for Scientific Research on Bioethics and Biosafety of the Instituto Mexicano del Seguro Social (IMSS) approved the experimental procedures under registration number R-2015-785-116 (approval date November 30, 2015) and R-2017-3603-33 (approval date June 5, 2017). For all the anesthesia procedures, a mixture of xylazine (10 mg/kg, PiSA, México city, México) and ketamine (50 mg/kg, PiSA) was intramuscularly (i.m.) applied to the hind limb of animals. When required, 0.063 g of sodium pentobarbital in 1 mL vehicle (Pisapental, PiSA, México city, México) was intramuscularly injected in the animals that required to be euthanized).

Animals

Sample size for this experiment was calculated using an alpha value of 0.05 and beta value of 0.20. Forty-eight female Sprague-Dawley rats, aged 12–15 weeks, weighing 230–250 g, were provided by the Animal Facility of the Proyecto Camina A.C. and included in this study.

Six groups ($n = 8$ rats/group) were used (GraphPad QuickCalcs: <http://www.graphpad.com/quickcalcs/>): 1) Sham (without SCI induction, and no treatment), 2) PBS (SCI induction, phosphate buffered saline intervention), 3) MLIF + A91 (SCI

induction, MLIF and A91 intervention), 4) MLIF + GSH-MEE (SCI induction, MLIF and GSH-MEE intervention), 5) A91 + GSH-MEE (SCI induction, A91 + GSH-MEE intervention), and 6) MLIF + A91 + GSH-MEE (SCI induction, MLIF, A91 and GSH-MEE intervention). After SCI, rats were housed in cages with good and water *ad libitum* under a 12-hour light/dark cycle at 21–23°C. All rats were subjected to manual bladder voiding, three times a day for 2 weeks. Sterile bedding and filtered water were replaced daily. In order to avoid infection, Enrofloxacin (Marvel, México City, México) was diluted into their drinking water at 64 mg/kg/day for 1 week. These animals were carefully monitored for signs of infection, dehydration, or auto mutilation with appropriate veterinary assistance as needed.

Spinal cord injury

The animals were anesthetized, and 30 minutes later, the thoracolumbar area was shaved, antiseptically prepared with iodopovidone, and a laminectomy was performed by removing the lamina at the thoracic vertebra 9 (T9) level to expose the spinal cord. A moderate injury was induced by dropping a 10 g cylinder from a height of 25 mm directly on the spinal cord using the NYU impactor (NYU, New York, NY, USA). The corresponding treatment was applied, and the muscle and skin were repaired with absorbable sutures (polyglycolic acid) and 4/0 and 3/0 nylon wire, respectively.

After treatment, specific care was provided, including verification of the persistence of neurogenic bladder function, manual emptying of the bladder three times a day, administration of 10% Enroxil antibiotic (5 mg/kg body weight) in drinking water and oral paracetamol (100 mg/kg body weight). In case of abscess formation at the surgical site, the area was debrided with the application of a disinfectant solution.

Preparation and administration of peptides

Immediately after SCI induction, 50 µL MLIF (44 µg/µL in PBS, pH = 7.4; American Peptide Company Co., Sunnyvale, CA, USA) or PBS was applied directly to the site of injury and then 50 µL MLIF or PBS was intraperitoneally administered three times, once every 24 hours (Bermeo et al., 2013).

One hour after SCI induction, 150 µg of A91 (1 µg/µL PBS; Invitrogen Life Technologies, San Diego, CA, USA) or emulsified PBS in an equal volume of Freund's complete adjuvant (Sigma, St. Louis, MO, USA) containing 0.5 mg/mL of mycobacterium tuberculosis (Ibarra et al., 2010; Garcia et al., 2012) was subcutaneously injected at the base of the tail.

After SCI induction, 12 mg/kg of GSH-MEE (Sigma) diluted in 0.8 mL saline solution was intraperitoneally administered as follows: the first dose of 4 mg/kg GSH-MEE was administered at 20 minutes after SCI, and the remaining 8 mg/kg GSH-MEE were divided into three equivalent doses (2.66 mg/kg), which were applied 4, 10, and 20 hours after SCI, respectively (Guizar-Sahagun et al., 2005).

Motor function recovery assessment

After SCI and treatment, double-blind evaluation was performed every 7 days for a period of 8 weeks. Motor function recovery was rated on a scale of 0 (complete paralysis) to 21 (complete mobility). Each rat was individually placed for 4 minutes in an open field of 1.5 m × 1.5 m, and movement recovery of the hip, knee, and ankle was evaluated using the Basso, Beattie and Bresnahan (BBB) locomotor rating scale (Basso et al., 1995). After the 8-week motor function evaluation period, four rats in each group were used to prepare spinal cord tissue sections, and the other four rats were used to prepare paraffin tissue sections.

Tissue procurement

After the last BBB evaluation, the animals were sedated with sodium pentobarbital (100 mg/kg), and 1000 U of heparin

was intraperitoneally delivered. Thoracotomy and intracardiac infusion were performed with a peristaltic pump (Thermo Fisher, Waltham, MA, USA). 250 mL of PBS, followed by 250 mL of 4% paraformaldehyde and 30% sucrose in PBS (pH 7.4) were administered at 4°C. A tissue segment of 1.8 cm was extracted from the central lesion zone of the spinal cord and kept overnight in the same fixative. The tissue was then transferred to 30% sucrose for 5 days at 4°C.

Procedure for spinal cold cuts

The tissues were placed in Tissue-Tek mounting medium (Sakura, Dubai, United Arab Emirates) and frozen at –20°C. Longitudinal sections were cut on a cryostat (Leica Biosystems). The first four 5 µm-thick sections were used to determine the deposition of collagen (Masson's trichrome staining). The following four 5 µm-thick sections were used for determining spinal cord parenchyma preservation [hematoxylin and eosin staining (H&E)], and the final four 40 µm-thick sections were used to determine axonal fibers (immunohistochemical staining) using the ependymal canal as a reference.

For histological staining (H&E and Masson's trichrome staining), the tissues were placed on slides loaded with poly-L-lysine (Sigma), fixed at 70°C/5 seconds, and dehydrated with distilled water, 70% ethanol/1 minute, 96% ethanol/1 minute, and absolute alcohol/1 minute. The slides were then placed in acetone for 10 minutes at 4°C and dried at room temperature. For immunohistochemical staining, the tissues were placed in 16-well plates containing 1 mL of PBS solution at 7.4 pH where the technique was carried out by flotation.

Procedure for paraffin sections

To determine ventral horn motor neurons (H&E staining) and myelin preservation [Luxol Fast Blue staining (LFB)], the tissue was placed in a graded series of ethanol: 70%/24 hours, 96%/20 minutes, 96%/20 minutes, 100%/30 minutes, and finally xylol/30 minutes. The dehydrated tissue was embedded in paraffin at 56°C for 2 hours and included in cassettes (Metrix Lab, México city, México). Serial cross-sections, 3 µm thick, were cut using a microtome (Leica Biosystems, Richmond, USA). Using the site of injury as a reference, sections were cut at 0.1 cm, 0.2 cm, 0.3 cm, 0.4 cm, and 0.5 cm in both the rostral and caudal directions from the epicentre of the lesion. The sections were placed on slides loaded with poly-L-lysine and dried at 70°C for 30 minute.

Preservation of the medullary parenchyma and ventral horn motor neurons (H&E)

The samples were hydrated as follows: Xylol (cold cuts, the tissue did not pass through this solvent), alcohol: absolute/30 seconds, 96%/30 seconds, 70%/30 seconds and distilled water/30 seconds.

The slides were placed in Harris hematoxylin for 5 minutes, washed with distilled water, washed twice with 0.1% absolute alcohol-hydrochloric acid, and washed again with distilled water. Five baths were made in 0.5% lithium carbonate and one bath in distilled water. The samples were stained with 0.5% Eosin for 30 seconds, dehydrated in an inverse manner (distilled water-Xylol). The slides were mounted with Entellan (Merck Millipore, México City, México), a coverslip was placed on the tissue, and finally, the total tissue was scanned. Images were captured at 2× and 20× magnifications with an Aperio microscope (Leica Biosystems, Chicago, IL, USA).

To determine the preservation of the medullary parenchyma in longitudinal sections, an area of 1 cm (0.5 cm rostral/0.5 cm caudal to the site of injury) was delimited and normalized to the pixel density obtained with respect to uninjured tissue (Sham group) using ImageJ v150B software (NIH, Bethesda, MD, USA).

Research Article

For ventral horn neurons in cross-sections, sections corresponding to tissue in quadrants were delimited with the Fiji tool of ImageJ software, and only cells in which the nucleus could be delimited were counted in the area 0.5 cm rostral/0.5 cm caudal to the site of injury.

White matter determination (Luxol Fast Blue staining)

The samples were hydrated in the following order: Xylol/30 seconds, alcohol: absolute/30 seconds, 96%/30 seconds, 70%/30 seconds, and distilled water/30 seconds. The slides were placed in 0.1% LFB solution/2 minutes and rinsed with distilled water. Then, the slides were washed 20–30 times in 0.05% lithium carbonate solution, which was freshly prepared, until the white matter (blue color) was differentiated from the grey matter, and the samples were then rinsed with distilled water. The tissue was placed in the cresyl violet solution for 4 minutes and dehydrated in an inverse manner (distilled water-xylol). The slides were mounted with Entellan (Merck Millipore), a coverslip was placed on the tissue, and images (2x and 20x) were captured with a Leica Aperio microscope by total tissue scanning.

To determine the preservation of myelin, the white matter and the grey matter were delimited with the ImageJ software; the grey matter pixels were subsequently discarded by adjusting the saturation percentage of the density at the bottom to 80% and adjusting the pixel units to 1 mm to analyze the area of each tissue sample. The sections were evaluated at 0.5 cm rostral/0.5 flow rate (every 0.1 cm) from the epicentre of the lesion.

Collagen deposition determination (Masson's trichrome staining)

To determine collagen deposition, the blue-dyed area representing the glial scar was delimited and, adjusting the pixel unit to 1 mm, Masson's trichrome-stained area in each tissue was analysed with ImageJ software.

The samples were hydrated in a graded series of alcohol as follows: absolute/30 seconds, 96%/30 seconds, 70%/30 seconds and distilled water/30 seconds. The samples were placed in Bouin's solution for 40 minutes, washed with running water, and then bathed with distilled water. They were placed in Weigert's hematoxylin solution for 10 minutes, washed with running water, and then bathed with distilled water. The samples were then placed in Biebrich scarlet solution for 10 minutes, washed with distilled water, placed in phosphotungstic acid-phospholimbic acid solution for 15 minutes and placed in aniline blue solution for 2 minutes. They were rinsed in distilled water and a 1% acetic acid bath. Slides were assembled with Entellan (Merck Millipore), placing a coverslip on the tissue, and images were captured at 0.8 × magnification with a Leica Aperio microscope through total tissue scanning.

To determine the presence of collagen, blue-stained area was delimited, and by adjusting the pixel unit to 1 mm, blue-stained on each tissue sample was analysed with ImageJ software.

Axonal fibre detection (immunohistochemistry flotation)

The obtained sections were placed in 16 well-flat bottom plates containing 1 mL of PBS at 0.1 M and pH 7.4 under constant agitation during the whole process. Endogenous peroxidases were inactivated by incubation with 0.09% hydrogen peroxide for 15 minutes, washed three times for 15 minutes each with 0.1 M PBS, incubated in epitope unmasking solution [(1× Immunoscreen) (BioSB, Santa Barbara, CA, USA)], dried at 70°C for 30 minutes, washed three times for 15 minutes each with 0.1 M PBS, incubated with the primary antibody [chicken anti-rat neurofilament H antibody; Cat# AB5539 (Merck Millipore)] in a 1:1000 dilution overnight at 4°C, and washed three times for 15 minutes each with 0.1 M

PBS/0.3% Triton solution. The sections were then incubated with the secondary antibody [rabbit anti-IgG-HRP antibody AB6734 (Merck Millipore)] at 4°C for 1 hour at a 1:1000 dilution with PBS-Triton and washed three times for 15 minutes each with 0.1 M PBS/Triton and once with distilled water. Diaminobenzidine solution was used to monitor the development under a microscope (2–10 minutes). Once the expected background was obtained by contrasting with the well-defined neurofilament fibres, the reaction was stopped by addition of distilled water. The sections were placed on slides with poly-L-lysine (Sigma), covered with Entellan (Merck Millipore), placing a coverslip on the tissue, and images were captured at 40× magnification with a Leica Aperio microscope through total tissue scanning.

To determine the amount of axonal fibres, the site of injury in the tissue section was located and delimited with parallel lines 0.5 cm rostral/0.5 caudal to the site of injury. Fibres were counted from top to bottom so as not to count the same axon twice. A marked axon was defined as the axon presenting well-defined dark brown colouration protruding from the bottom. The images were scanned using the free access software ImageJ v1.50B.

Statistical analysis

The groups were descriptively analyzed to verify the distribution of data. Data are expressed as the mean ± SEM. Open field locomotion test and one-way analysis of variance (ANOVA) for repeated measures with Bonferroni's *post hoc* test were performed. Two-way ANOVA for repeated measures was performed to evaluate survival of ventral horn motor neurons and white matter preservation. One-way ANOVA with Tukey's *post hoc* test was performed to evaluate preservation of medullary parenchyma and axonal count. Kruskal-Wallis test followed by Mann-Whitney *U* test was performed to evaluate presence of collagen. The threshold for significance was defined as $P < 0.05$. GraphPad Prism 8 software (San Diego, CA, USA) was used to perform data analysis.

Results

Motor functional recovery of rats

The sham group had a BBB score of 21. SCI groups treated with different combinations of immunomodulatory peptides from the second post-injury week obtained better scores than the PBS-treated group. Nevertheless, the rats treated with three immunomodulatory peptides obtained the best scores with a maximum of 10.1 ± 0.4 points on the 8th week. This value was significantly higher than the one presented by A91 + GSH-MEE (8.7 ± 0.6 ; $F = 2.19$, $P = 0.04$; one-way ANOVA for repeated measures with Bonferroni's *post hoc* test), MLIF + A91 (7.6 ± 0.4 ; $F = 4.52$, $P = 0.005$), MLIF + GSH-MEE (7.6 ± 0.2 ; $F = 5.94$, $P < 0.001$) or PBS (4.9 ± 0.4 ; $F = 15.39$, $P < 0.0001$) groups (**Figure 1**).

Preservation of medullary parenchyma

Figure 2A shows representative spinal cord sections from each of the H&E-stained groups. The MLIF + A91 + GSH-MEE group presented the most complete tissue. The percentage of preserved tissue is presented in **Figure 2B**, with the Sham group at the T9 level taken as a reference corresponding to 100% integrity with the same caudal and rostral length. The percentage of preserved tissue in SCI rats was higher in the MLIF + A91 + GSH-MEE (67.5 ± 1) than that in the other groups: A91+ GSH-MEE (62.5 ± 0.8), MLIF + A91 (60.2 ± 1), MLIF + GSH-MEE (58.9 ± 0.7) and PBS (55.9 ± 1.4 ; $F = 17.91$, $P < 0.001$).

Ventral horn motor neurons

Figure 3A shows representative H&E stained spinal cord sections, which were taken at 0.5 cm cranial and 0.5 cm caudal to the epicentre of the lesion in each group. Fewer

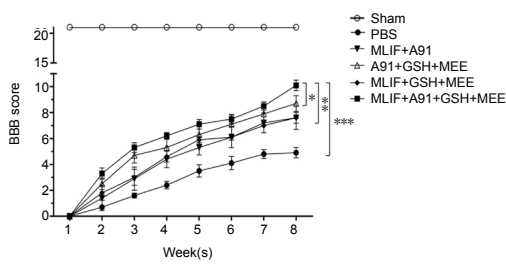


Figure 1 | Open field test for evaluation of motor function.

The MLIF + A91 + GSH-MEE group showed better motor function recovery at the end of the observation period. $*P < 0.05$, $**P < 0.01$, $***P < 0.0001$. One-way analysis of variance for repeated measures with Bonferroni's *post hoc* test. The data are presented as the mean \pm SEM of eight rats per group. BBB: Basso, Beattie and Bresnahan locomotor rating scale; GSH-MEE: glutathione monoethyl ester; MLIF: monocyte locomotion inhibitor factor; PBS: phosphate buffer saline.

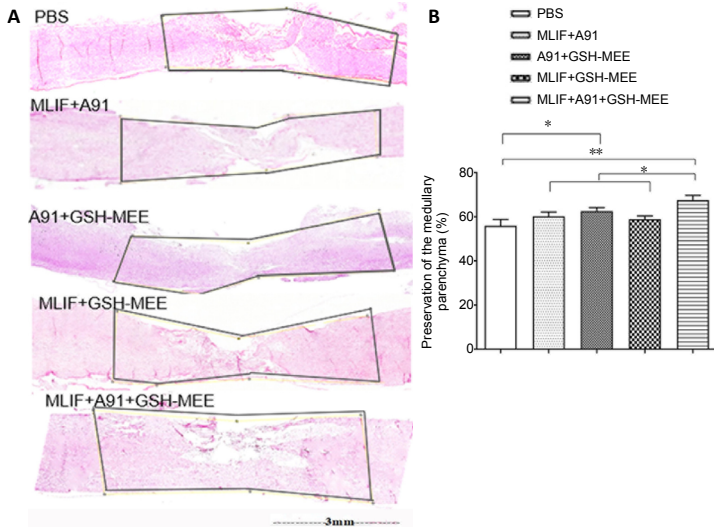


Figure 2 | Preservation of the medullary parenchyma 8 weeks after spinal cord injury.

(A) Representative hematoxylin & eosin-stained samples of each group, taken 0.5 cm rostral to and 0.5 cm caudal to the epicenter of the lesion, which are shown to determine the percentage of preserved tissue. (B) Graphic representation of the percentage of preservation relative to the sham group. A higher percentage of preserved tissue in the group treated with the combined therapy of MLIF, A91 and GSH-MEE was observed. One-way analysis of variance with Tukey's *post hoc* test ($*P < 0.05$, $**P = 0.001$). The data are presented as the mean \pm SEM of four rats per group. GSH-MEE: Glutathione monoethyl ester; MLIF: monocyte locomotion inhibitor factor.

residual motoneurons of the ventral horn (capable of innervating posterior tracts, evidenced by the Nissl-stained nuclei) were observed in the PBS group than in the MLIF + A91 + GSH-MEE group. The graphical analysis (**Figure 3B**) shows that there was no significant difference in the cell count at the cranial level among the SCI groups. However, cell count at the caudal level in the MLIF + A91 + GSH-MEE group was significantly higher than that in the PBS group ($F = 6.60$, $P = 0.0001$) and that in the MLIF + A91, A91 + GSH-MEE, MLIF + GSH-MEE groups ($F = 1.82$, $P = 0.01$). There was no significant difference in the cell count at the caudal level among PBS, MLIF + A91, and MLIF + GSH-MEE groups, and significant difference was compared when compared with the PBS group ($F = 1.98$, $P = 0.005$).

Preservation of white matter (myelin)

Figure 4A shows representative LFB-stained samples of each group. Dark blue colouration was observed in the white matter, which is defined as functional myelin attached to the axons. **Figure 4B** shows the densitometric analysis (every 0.1 cm). There was no significant difference in preservation of white matter at the cranial level among MLIF + A91, MLIF + GSH-MEE, A91 + GSH-MEE, and MLIF + A91 + GSH-MEE groups. The preservation of white matter at the caudal level in the MLIF + A91 + GSH-MEE group was significantly higher than that in the PBS ($F = 5.06$, $P < 0.001$) and MLIF + A91, MLIF + GSH-MEE, A91 + GSH-MEE groups ($F = 2.61$, $P < 0.05$). There was no significant difference in preservation of white matter at the caudal level among MLIF + A91, MLIF + GSH-MEE, and A91 + GSH-MEE groups, but significant difference was found between MLIF + A91, MLIF + GSH-MEE, and A91 + GSH-MEE groups and PBS group ($F = 3.46$, $P < 0.01$).

Collagen deposition at the site of injury

Figure 5A shows representative Masson's trichrome-stained samples depicting collagen deposition (in blue) at the site of injury. **Figure 5B** shows the densitometric analysis of each group. The MLIF + A91 + GSH-MEE group presented a significant reduction of collagen deposition as compared to the PBS, MLIF + A91, MLIF + GSH-MEE, and A91 + GSH-MEE groups ($P < 0.0001$, $P < 0.05$, respectively). The MLIF + A91, MLIF + GSH-MEE, and A91 + GSH-MEE groups exhibited a significantly lower amount of deposited collagen as compared to the PBS group ($P < 0.01$).

The number of axons

Figure 6A shows representative images of the spared axons at the rostral and caudal regions of each group. **Figure 6B** shows the counts of axonal fibres.

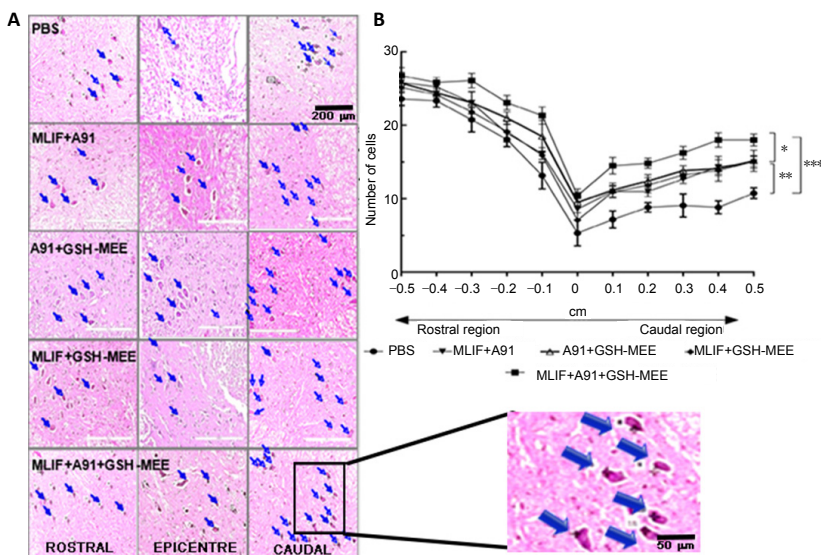


Figure 3 | The number of motor neurons of the residual ventral horn.

(A) Hematoxylin-eosin staining: The arrows indicate some motor neurons in each group (representative) at the epicentre of the lesion and at 0.5 cm rostral to and 0.5 cm caudal to the epicenter of the lesion. (B) Graphical representation of the number of motor neurons in each group in the rostral and caudal regions (every 0.1 cm). Two-way repeated measures analysis of variance was performed to reveal the difference among the groups. The data are presented as the mean \pm SEM of four rats per group. $*P = 0.01$, $**P = 0.005$, $***P = 0.0001$. GSH-MEE: Glutathione monoethyl ester; MLIF: monocyte locomotion inhibitor factor.

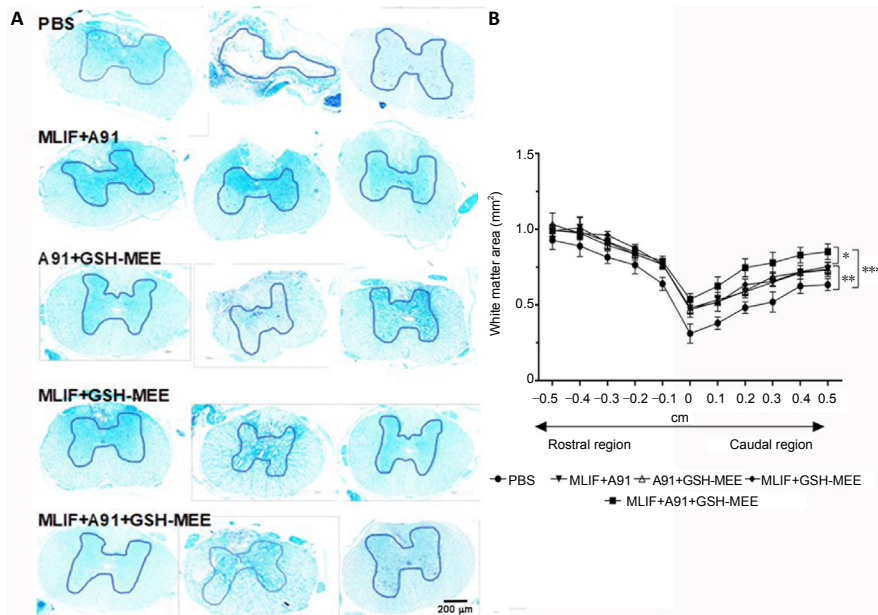


Figure 4 | Determination of preserved myelin. (A) Histological representation of sections of rats in each group. Outlines depict the exact myelinated assessed area. From left to right, sections represent proximal (0.5 cm), epicenter and distal (0.5 cm) segments. (B) Determination of the area (in mm²) of white matter (every 0.1 cm). Two-way analysis of variance for repeated measures revealed that there was significant difference in preserved myelin in the epicenter of the lesion (0 cm) between MLIF + A91 + GSH-MEE group and the PBS group. The data are presented as the mean ± SEM of four rats per group. **P* < 0.05, ***P* < 0.01, ****P* < 0.001.

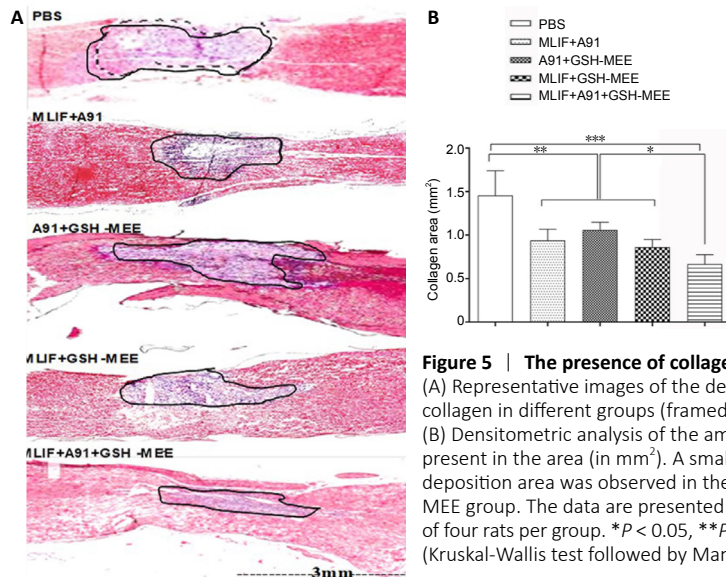


Figure 5 | The presence of collagen. (A) Representative images of the deposition of collagen in different groups (framed by black line). (B) Densitometric analysis of the amount of collagen present in the area (in mm²). A smaller collagen deposition area was observed in the MLIF + A91 + GSH-MEE group. The data are presented as the mean ± SEM of four rats per group. **P* < 0.05, ***P* < 0.01, ****P* < 0.001 (Kruskal-Wallis test followed by Mann-Whitney *U* test).

Axons were counted at the rostral (0.5 cm), epicentre and caudal (0.5 cm) regions. The number of fibers at the lesion epicentre and at the caudal level in the MLIF + A91 + GSH-MEE group was significantly higher than that in the PBS group (*F* = 3.03, *P* = 0.049, and *F* = 4.2, *P* < 0.01, respectively). The number of axons, but only at the caudal level, in the MLIF + A91 + GSH-MEE group was significantly higher than that in the MLIF + A91, MLIF + GSH-MEE, and A91 + GSH-MEE groups (*F* = 4.3, *P* = 0.02). The number of axons at the caudal level in the MLIF + A91, MLIF + GSH-MEE, and A91 + GSH-MEE groups was significantly higher than that in the PBS group (*F* = 4.05, *P* = 0.03).

Discussion

Previous studies have demonstrated that individual application of MLIF or GSH-MEE acts against destructive phenomena from the beginning of SCI. A91 peptide exerts its protective effect starting from 4–6 days after injury (Guizar-Sahagun et al., 2005; Ibarra et al., 2013; Bermeo et al., 2015). This attractive two-phase effect incited our research group to evaluate the effect of the three-peptide therapy on motor functional and morphological recovery. Based on the results of the individual action of each of these peptides, we can infer that the application of the proposed combination is synergistic and favors motor functional recovery more effectively than individual or dual treatments (Guizar-Sahagun et al., 2005; Martiñon et al., 2007; Bermeo et al., 2015).

The proposed three-peptide therapy potentiated motor functional recovery and also promoted neuroprotection. Regarding the latter, individual therapy with any of the peptides used in this work has shown neuroprotective effects by inhibiting apoptosis, lipid peroxidation, inflammation or even nitric oxide production (Guizar-Sahagun

et al., 2005; Ibarra et al., 2010; Rodriguez-Barrera et al., 2013; Bermeo et al., 2015; Garcia et al., 2018). These beneficial effects have favored the preservation of neural tissue. For instance, studies by our group have shown that the three peptides (each one per separate) have a protective effect on red nucleus neurons that project axons below the site of injury that favor motor functional recovery (Martiñon et al., 2007; Bermeo et al., 2015). The combined strategy used in this work, could then, support the preservation of this and other descending pathways, which together with the quantity and quality of the preserved tissue are essential in explaining the observed functional improvement.

In the present study, the three-peptide strategy also exhibited a significant protective effect on myelin, which was greater than that observed in the other experimental groups. This beneficial effect could be induced, at least in part, by inhibiting lipid peroxidation, one of the main destructive phenomenon

triggered after injury. With this respect, the central nervous system has been shown to exhibit a low antioxidant capacity (Profyris et al., 2004; Visavadiya et al., 2016) and high concentrations of polyunsaturated fatty acids (main target of the free radicals) in such a way that, it is not able to attenuate the oxidative response after mechanical damage.

The overproduction of free radicals occurs during the first 5 hours after injury (Rodriguez-Barrera et al., 2020); thus, the administration of MLIF and GSH-MEE covers this peak in free radical production. Afterwards, the myelin is attacked by other waves of free radicals, generating oxidative damage, thus propagating as a constant cycle of damage that expands throughout the injury (Hall et al., 2016; Hilton et al., 2017). At this time, the proposed treatment has the ability to neutralize these reactive species since A91-immunization likely exerts its inhibitory effect on lipid peroxidation (Figure 7). Therefore, the three peptides used this study play an

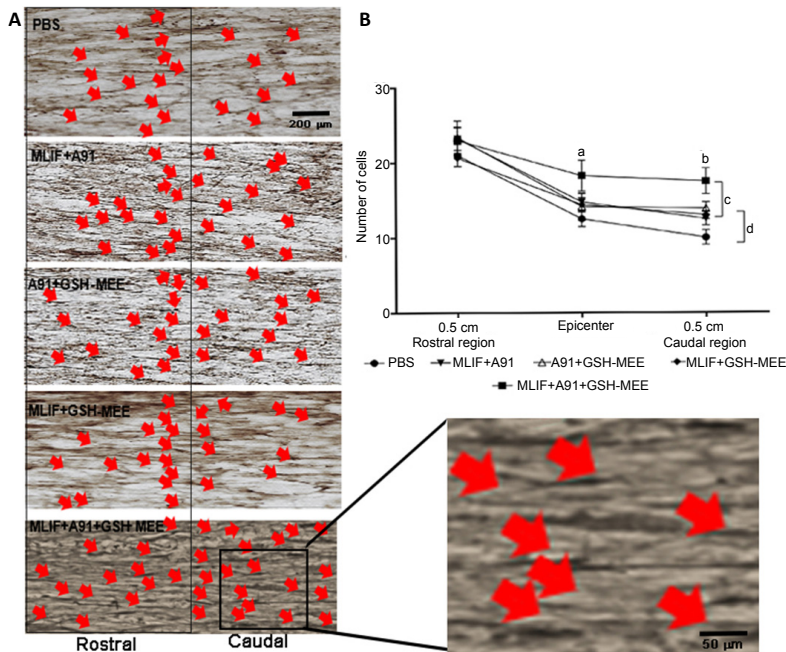


Figure 6 | Number of axons at different levels of the spinal cord.

(A) Immunohistochemical results of axonal fibres (red arrows) in the spinal cord at the rostral and caudal regions. (B) Graphical representation of the axonal counts at proximal, epicenter and caudal levels. Significant difference in axons at the epicentre and caudal levels of injury was observed between the MLIF + A91 + GSH-MEE group and other groups. The data are presented as the mean \pm SEM of four rats per group. ^a $P = 0.049$, vs. PBS group; ^b $P = 0.01$, vs. PBS group; ^c $P = 0.02$, MLIF + A91 + GSH-MEE group vs. MLIF + A91, A91 + GSH-MEE or MLIF + GSH-MEE group; ^d $P = 0.03$, MLIF + A91, A91 + GSH-MEE or MLIF + GSH-MEE group vs. PBS group. Immunohistochemistry was performed using the rat anti-neurofilament H as the primary antibody. GSH-MEE: Glutathione monoethyl ester; MLIF: monocyte locomotion inhibitor factor; PBS: phosphate buffer saline.

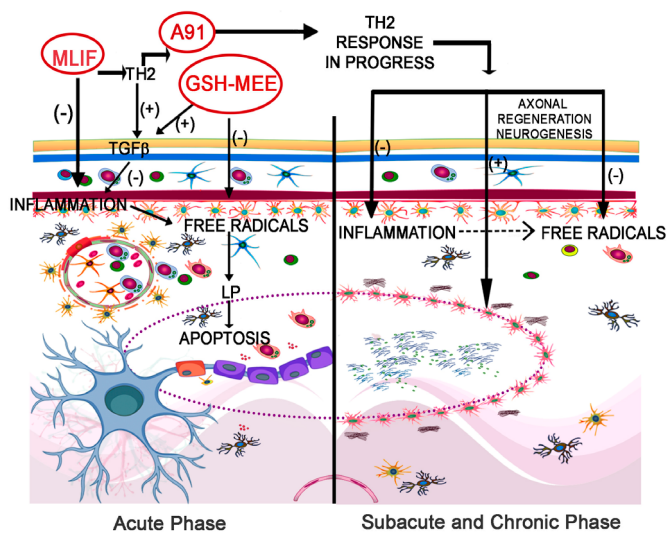


Figure 7 | Mechanisms of the combined therapy of MLIF, A91 and GSH-MEE.

From acute to subacute and chronic phases, the three-peptide therapy exerts its beneficial effects. MLIF and GSH-MEE protect neural tissue by upregulating (+) the expression of the transforming growth factor-beta (TGF- β) and then diminishing (-) inflammation, lipid peroxidation (LP) and apoptosis. Furthermore, these peptides support the activation of T cells towards an anti-inflammatory phenotype (TH2). Likewise, MLIF and GSH-MEE enhance the anti-A91 response, which will protect and restore neural tissue during the subacute and chronic phases. A91 peptide: The immunodominant epitope of sequence 87–99 of the myelin basic protein with a lysine substituted by an alanine at position 91 (Val-His-Phe-Phe-Ala-Asn-Ile-Val-Thr-Pro-Arg-Thr-Pro); GSH-MEE: Glutathione monoethyl ester [γ -Glu-Cys-Gly-OEt]; MLIF peptide: monocyte locomotion inhibitor factor [Met-Gln-Cys-Asn-Ser].

important role as antioxidants to eliminate or decrease these reactive species and then lipid peroxidation, favoring the preservation of myelin (Profyris et al., 2004; Guizar-Sahagun et al., 2005; Rodriguez-Barrera et al., 2013; Bermeo et al., 2015; Garcia et al., 2018). Previous studies have shown that the administration of GSH-MEE and MLIF or analogues thereof provides neuroprotection after cerebral ischemia and significantly decreases lipid peroxidation after trauma (Bermeo et al., 2015; Kilanczyk et al., 2016; Vilchis et al., 2019).

At 14 days after injury, formation of glial scar begins with collagen synthesis (Wang et al., 2017). Our results showed

that the area of collagen deposition was slightly decreased in the groups receiving combined treatments, in particular in the group treated with three-peptide therapy. It is worth mentioning that both MLIF and A91 peptides provide an anti-inflammatory environment with a Th2 phenotype capable of diminishing glial scar. Therefore, the combination of these therapeutic strategies contributed to greater reduction of glial scar. This beneficial effect favors the possibility of a functional axonal regeneration, a possible effect that should be further investigated (Vilchis et al., 2019).

Neurofilaments are part of axonal cytoskeleton. They provide mechanical strength and stability and determine the diameter of axons, ensuring that the axons that meet the intact cytoskeleton are functional. In this investigation, we immunolabelled the axonal neurofilaments and determined the number of axonal fibres at the caudal and rostral regions of the SCI animals. A positive effect on the number of axons was observed for treatment with the peptides, but a significant difference in the number of these fibres was observed in the group treated with the triple therapy compared with the PBS group and the dual-treatment groups.

It is anticipated that the increased number of axons in the peptide-treated groups is attributable to the neuroprotective effect exerted by the treatment; however, especially at the caudal stump of the spinal cord it is likely the result of an axon regeneration process. Previous studies have reported that at least A91 peptide is capable of modulating the expression of neurotrophic factors and the formation of regenerating axons (Kilanczyk et al., 2016; Wang et al., 2017; Nathan and Li, 2017; Garcia et al., 2019). Therefore, we can infer that this modulatory effect could also participate, at least in part, in restorative process and thus, in neurological functional recovery of SCI rats. This preliminary investigation includes only one evaluation of functional recovery, and thus, to strength the findings, future studies should consider more clinical and also electrophysiological assessments.

In conclusion, the results obtained indicate that MLIF + A91 + GSH-MEE therapy favors preservation of the medullary parenchyma, ventral horn, motor neurons, myelin, and the number of axonal fibers. Furthermore, it decreases the deposition of collagen, contributing to the pass of possible regenerating axons through the epicentre of lesion. Together, these beneficial effects can explain the better motor function recovery of rats in the MLIF + A91 + GSH-MEE group.

Research Article

This neuroprotective strategy is useful not only for SCI, but also for other neurodegenerative and neuroinflammatory acute or chronic pathologies, such as cerebral ischemia, circulatory shock, chronic inflammation, other traumatic injuries, or diseases in which the CNS is damaged by infectious agents such as bacteria, viruses, and protozoa. The use of a combined strategy of immunomodulatory peptides contributes to a better functional recovery.

Author contributions: *DPV and JVV contributed to the design of experiments, and substantially to the acquisition, analysis and interpretation of data. JHG, LBE, AFR, ATZ and EG contributed to the acquisition and interpretation of data, surgical procedures and postoperative care of experimental animals. EG contributed to the conception and design of this project and the writing of the manuscript. KSZ and RBR contributed to data acquisition, material preparation and postoperative care. RSG and AI contributed to the acquisition of funds and resources, the conception and design of this project, the general supervision of the research group, the writing of the manuscript and gave the final approval of this manuscript. All authors read and approved the final manuscript attributed to data acquisition and postoperative care.*

Conflicts of interest: None declared.

Financial support: *This study was supported by Fondo de Investigación en Salud of the Instituto Mexicano del Seguro Social (IMSS), under the support No. FIS/IMSS/PROT/G17/1676 and FIS/IMSS/PROT/G18/1825 and the scholarship granted to the students of Master's degree by Consejo Nacional de Ciencia y Tecnología (CONACYT) and IMSS. The funders had no role in study design, data collection and analysis, decision to publish, or preparation of the manuscript.*

Institutional review board statement: *This study was approved by the National Commission for Scientific Research on Bioethics and Biosafety of the Instituto Mexicano del Seguro Social under registration number R-2015-785-116 (approval date November 30, 2015) and R-2017-3603-33 (approval date June 5, 2017).*

Copyright license agreement: *The Copyright License Agreement has been signed by all authors before publication.*

Data sharing statement: *Datasets analyzed during the current study are available from the corresponding author on reasonable request.*

Plagiarism check: *Checked twice by iThenticate.*

Peer review: *Externally peer reviewed.*

Open access statement: *This is an open access journal, and articles are distributed under the terms of the Creative Commons Attribution-NonCommercial-ShareAlike 4.0 License, which allows others to remix, tweak, and build upon the work non-commercially, as long as appropriate credit is given and the new creations are licensed under the identical terms.*

References

Bains M, Hall ED (2012) Antioxidant therapies in traumatic brain and spinal cord injury. *Biochim Biophys Acta* 1822:675-84.

Basso DM, Beattie MS, Bresnahan JC (1995) A sensitive and reliable locomotor rating scale for open field testing in rats. *J Neurotrauma* 12:1-21.

Bermeo G, Ibarra A, Garcia E, Flores-Romero A, Rico-Rosillo G, Marroquin R, Mestre H, Flores C, Blanco-Favela F, Silva-García R (2015) Monocyte locomotion inhibitory factor produced by E. histolytica improves motor recovery and develops neuroprotection after traumatic injury to the spinal cord. *Biomed Res Int* 2013:340727.

Bloom O, Herman PE, Spungen AM (2020) Systemic inflammation in traumatic spinal cord injury. *Exp Neurol* 325:113143.

Chen X, Zhu W (2016) A mathematical model of regenerative axon growing along glial scar after spinal cord injury. *Comput Math Methods Med* 2016:3030454.

Dalbayrak S, Yaman O, Yilmaz T (2015) Current and future surgery strategies for spinal cord injuries. *World J Orthop* 6:34-41.

del Rayo-Garrido M, Silva-García R, García E, Martinon S, Morales M, Mestre H, Flores-Domínguez C, Flores A, Ibarra A (2013) Therapeutic window for combination therapy of A91 peptide and glutathione allows delayed treatment after spinal cord injury. *Basic Clin Pharmacol Toxicol* 112:314-318.

Faden AI, Stoica B (2007) Neuroprotection: challenges and opportunities. *Arch Neurol* 64:794-800.

Fitch MT, Silver J (2008) CNS injury, glial scars, and inflammation: Inhibitory extracellular matrices and regeneration failure. *Exp Neurol* 209:294-301.

García E, Rodríguez-Barrera R, Buzoianu-Anguiano V, Flores-Romero A, Malagon-Axotla E, Guerrero-Godínez M, De la Cruz-Castillo E, Castillo-Carvajal L, Rivas-González M, Santiago-Tovar P, Morales I, Borlongan C, Ibarra A (2019) Use of a combination strategy to improve neuroprotection and neuroregeneration in a rat model of acute spinal cord injury. *Neural Regen Res* 14:1060-1068.

García E, Silva-García R, Flores-Romero A, Blancas-Espinoza L, Rodríguez-Barrera R, Ibarra A (2018) The severity of spinal cord injury determines the inflammatory gene expression pattern after immunization with neural-derived peptides. *J Mol Neurosci* 65:190-195.

García E, Silva-García R, Mestre H, Flores N, Martinon S, Calderon-Aranda ES, Ibarra A (2012) Immunization with A91 peptide or copolymer-1 reduces the production of nitric oxide and inducible nitric oxide synthase gene expression after spinal cord injury. *J Neurosci Res* 90:656-663.

Guizar-Sahagun G, Ibarra A, Espitia A, Martínez A, Madrazo I, Franco-Bourland RE (2005) Glutathione monoethyl ester improves functional recovery, enhances neuron survival, and stabilizes spinal cord blood flow after spinal cord injury in rats. *Neuroscience* 130:639-649.

Hall ED, Wang JA, Bosken JM, Singh IN (2016) Lipid peroxidation in brain or spinal cord mitochondria after injury. *J Bioenerg Biomembr* 48:169-174.

Hille B, Catterall WA (1999) Electrical excitability and ion channels. In: *Basic neurochemistry: molecular, cellular and medical aspects* (Siegel GJ, Agranoff BW, Albers RW, eds), pp 95-110. Philadelphia: Lippincott-Raven.

Hilton BJ, Moulson AJ, Tetzlaff W (2017) Neuroprotection and secondary damage following spinal cord injury: concepts and methods. *Neurosci Lett* 652:3-10.

Ibarra A, García E, Flores N, Martinon S, Reyes R, Campos MG, Maciel M, Mestre H (2010) Immunization with neural-derived antigens inhibits lipid peroxidation after spinal cord injury. *Neurosci Lett* 476:62-65.

Ibarra A, Sosa M, García E, Flores A, Cruz Y, Mestre H, Martiñón S, Pineda-Rodríguez BA, Gutiérrez-Ospina G (2013) Prophylactic neuroprotection with A91 improves the outcome of spinal cord injured rats. *Neurosci Lett* 554:59-63.

Kilanczyk E, Saraswat Ohri S, Whitemore SR, Hetman M (2016) Antioxidant protection of NADPH-depleted oligodendrocyte precursor cells is dependent on supply of reduced glutathione. *ASN Neuro* 8:1759091416660404.

Liesi P, Kaupilla T (2002) Induction of type IV collagen and other basement-membrane-associated proteins after spinal cord injury of the adult rat may participate in formation of the glial scar. *Exp Neurol* 173:31-45.

Martiñón S, García E, Flores N, González I, Ortega T, Buenrostro M (2007) Vaccination with a neural-derived peptide plus administration of glutathione improves the performance of paraplegic rats. *Eur J Neurosci* 26:403-412.

Moghaddam A, Child C, Bruckner T, Gerner HJ, Daniel V, Biglari B (2015) Posttraumatic inflammation as a key to neuroregeneration after traumatic spinal cord injury. *Int J Mol Sci* 6:7900-7916.

Nathan FM, Li S (2017) Environmental cues determine the fate of astrocytes after spinal cord injury. *Neural Regen Res* 12:1964-1970.

Oyinbo CA (2011) Secondary injury mechanisms in traumatic spinal cord injury: a nugget of this multiply cascade. *Acta Neurobiol Exp (Wars)* 71:281-99.

Profyris C, Cheema SS, Zang D, Azari MF, Boyle K, Petratos S (2004) Degenerative and regenerative mechanisms governing spinal cord injury. *Neurobiol Dis* 15:415-436.

Rodríguez-Barrera R, Fernández-Presas AM, García E, Flores-Romero A, Martinon S, González-Puertos VY, Mestre H, Flores-Domínguez C, Rodríguez-Mata V, Königsberg M, Solano S, Ibarra A (2013) Immunization with a neural-derived peptide protects the spinal cord from apoptosis after traumatic injury. *Biomed Res Int* 2013:827517.

Rodríguez-Barrera R, Flores-Romero A, García E, Fernández-Presas AM, Incontri-Abraham D, Navarro-Torres L, García-Sánchez J, Juárez-Vignon Whaley JJ, Madrazo I, Ibarra A (2020) Immunization with neural-derived peptides increases neurogenesis in rats with chronic spinal cord injury. *CNS Neurosci Ther* 26:650-658.

Rowland JW, Hawryluk GW, Kwon B, Fehlings MG (2008) Current status of acute spinal cord injury pathophysiology and emerging therapies: promise on the horizon. *Neurosurg Focus* 25:E2.

Vilchis J, Parra DM, Toscano JA, Blancas L, Herrera J, Silva R (2019) Current developments in antioxidant therapies for spinal cord injury. In: *Spinal cord injury therapy* (Ibarra A, ed), pp 1-32. UK: Intech.

Visavadiya NP, Patel SP, VanRooyen JL, Sullivan PG, Rabchevsky AG (2016) Cellular and subcellular oxidative stress parameters following severe spinal cord injury. *Redox Biol* 8:59-67.

Wang X, Wang C, Yang Y, Ni J (2017) New monocyte locomotion inhibitory factor analogs protect against cerebral ischemia-reperfusion injury in rats. *Bosn J Basic Med Sci* 17:221-227.

Wilson JR, Cronin S, Fehlings MG, Kwon BK, Badhiwala JH, Ginsberg H, Witwi C, Jaglal S (2020) The epidemiology and impact of spinal cord injury in the elderly: results of a 15-year population-based cohort study. *J Neurotrauma* 37:1740-1751.

Xu GY, Hughes MG, Ye Z, Hulsebosch CE, McAdoo DJ (2004) Concentrations of glutamate released following spinal cord injury kill oligodendrocytes in the spinal cord. *Exp Neurol* 187:329-336.

Co-Editor: Zhao M; S-Editor: Li CH; L-Editor: Song LP; T-Editor: Jia Y